Environ. Sci. Technol. **1998**, *32,* 1615−1622

Determination of Size-Dependent Dry Particle Deposition Velocities with Multiple Intrinsic Elemental Tracers

PETER F. CAFFREY† AND JOHN M. ONDOV*

Department of Chemistry and Biochemistry, University of Maryland, College Park, Maryland 20742

MARIA J. ZUFALL AND CLIFF I. DAVIDSON

Department of Civil and Environmental Engineering, Carnegie Mellon University, Pittsburgh, Pennsylvania 15213

Dry deposition flux and aerosol size distribution measurements were made concurrently aboard the RV *Lake Guardian* 19 km east of the Chicago shoreline during summer 1994 to assess atmospheric inputs of minor and trace elements to southern Lake Michigan. Size-segregated aerosol measurements were made over consecutive 12-h periods with Micro-Orifice and Noll Rotary impactors (MOI and NRI), and depositing-particulate collections to aerodynamically smooth airfoils were made over periods of 3−4 days. The combination of the MOI and NRI provided size-segregated particulate samples in 12 discrete intervals between 0.059 and, nominally, 100 μm. The samples were analyzed for As, Ca, Mg, Se, Sb, V, and Zn by instrumental neutron activation analysis and for S by X-ray fluorescence. Aerosol and deposition data for individual elemental constituents were fit with a chemical mass balance deposition (CMBD) model in which a set of particle-size-specific deposition velocities (V_d), best reconciling the deposition data, were determined by iterative (constrained) solution of a series of six linear equations using the Levenberg−Marquardt method. Under stable conditions and mean wind speed of 4.0 m s^{-1}, minimum V_d values for particles with physical diameters between 0.09 and 0.53 μm averaged 0.006 ± 0.005 cm s^{-1}, wherein uncertainties were determined by Monte Carlo analysis. This agrees favorably with values determined by microscopy for which uncertainties were much larger and with those predicted by the Williams model for the same period. The results suggest that physically significant V_d values are obtainable from a constrained CMBD model.

Introduction

Dry deposition of atmospheric aerosol particles is thought to be an important pathway for the introduction of toxic trace elements and heavy metals (*2*); polynuclear aromatic hydrocarbons (PAH) (*3*); and some pesticides (*4*) into the Great Lakes, especially for Lake Michigan, which lies in close proximity to the large urban and heavily industrialized Chicago/Gary area (*5*). However, dry deposition fluxes are difficult to measure and instead are often estimated as the product of the dry deposition velocity (V_d) and the corresponding areal pollutant concentration. The V_d strongly depends on particle size, meteorology (atmospheric stability, relative humidity, and wind speed), and characteristics of the depositing surface. In general, actual V_d measurements over water are few, are subject to large uncertainties, and are often reported for crudely sized aerosol fractions and for only a highly limited range of often poorly characterized meteorological conditions (*6*). Those calculated with models typically underestimate particulate V_d values (*7*). Overall, there remains a 2−3-fold uncertainty in V_d values and fluxes derived from these parameters (*7*). Thus, refinements in these determinations are critically needed to understand the true scope of dry deposition to Lake Michigan and other natural waters.

Holsen et al. (*8*) and Wu et al. (*9*) have recently employed smooth, wind-tunnel tested, surrogate surfaces to investigate spatial variations in dry deposition. These do not accurately simulate characteristics of natural water surfaces (*10*−*12*) for which surface roughness, white-cap formation, and humidity gradients (*13*) are thought to enhance deposition but can provide useful estimates of the minimum deposition rates to relatively calm water (*8*). These studies focused on the deposition of large particles, as they settle more rapidly than fine particles and often dominate dry deposition fluxes. However, fine-particle (i.e., those with aerodynamic diameters <2.5 μm) deposition is also important, as fine particles carry the bulk of the primary pollutants from high-temperature combustion sources (*14*) and have long atmospheric residence times. Smaller particles are, therefore, available for deposition to nearly the entire surface of lakes as large as Lake Michigan, where they can contribute substantially to the total, lakewide dry deposition rates (*15*).

In a companion paper in this issue, Zufall et al. (*1*) determined size-dependent V_d values for aerodynamic surrogate surfaces in the shape of symmetric airfoils. In their work, scanning electron microscopy (SEM) was used to count particles in 10 geometrically spaced intervals between 0.25 and >100 μm in both aerosol and deposition samples. Particle mass distributions were inferred from projected areas, and particle densities were estimated from semiquantitative energy-dispersive X-ray (EDX) detection. Herein, we apply a chemical mass balance deposition (CMBD) model to derive size-dependent V_d values for atmospheric particles to identical, collocated surrogate surfaces collected concurrently with those of Zufall et al. (*1*). Our intent was to calculate minimum V_d values using an independent method and with greater focus on the submicrometer aerosol than in previous studies. The results are compared with those reported by Zufall et al. (*1*) and those calculated with the Williams model (*16*) under the prevailing meteorological conditions. Both studies are part of the Atmospheric Exchange Over Lakes and Oceans (AEOLOS) project, initiated by the U.S. Environmental Protection Agency to assess the contributions of potentially important toxins to coastal water bodies from adjacent urban and industrial areas. Herein, suspended and deposited aerosol samples were collected at an urban site in Chicago, off-shore aboard a research vessel, and at a rural site on the eastern shore to assess the influence of aerosol deposition from urban and industrial sources affecting southern Lake Michigan. In the AEOLOS−Lake Michigan project, sampling occurred during three periods: 3 days in May 1994, 2 weeks in July 1994, and 3 days in January 1995. Results presented here were collected aboard ship during the July sampling

* Corresponding author phone: (301)405-1859; fax: (301)314-9121; e-mail: jondov@wam.umd.edu.

† Present address: Remote Sensing Division, Naval Research Lab Code 7228, Washington, DC 20375.

S0013-936X(97)00644-5 CCC: $15.00
Published on Web 04/24/1998

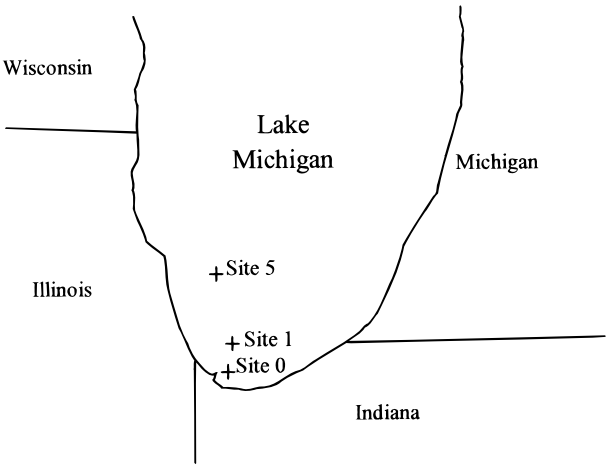

FIGURE 1. Schematic map of southern Lake Michigan showing offshore sampling locations.

campaign. Those in the companion paper by Zufall et al. (*1*) report results from two periods: July 1994 and January 1995.

Experimental Methods

Sampling. Samples discussed herein were collected over a 1-week period beginning July 21, 1994, with simultaneously operated nine-stage Micro-Orifice and four-stage Noll Rotary impactors (MOI and NRI, respectively) to produce a total of 13 size-segregated aerosol fractions for elemental analysis. In addition, dry deposition flux measurements were made using "Frisbee"-shaped symmetric airfoils (*9*, *17*), collected concurrently with the impactor samples. The MOI was equipped with an integral backup filter and operated at 30 $\pm$ 1 L min^{-1}, and the NRI was operated at a speed of 320 rpm. Fifty percent aerodynamic cutoff diameters (D_{50}) under these conditions were 15, 3.2, 1.8, 1.0, 0.55, 0.29, 0.17, 0.091, and 0.053 μm and 36.5, 24.7, 11.5, and 6.5 μm for the for the MOI (*18*) and NRI (*19*), respectively. The largest particles collected by the MOI and NRI impactors are assumed to be 30 and 100 μm (*19*), respectively. Gelman "Teflo" Teflon filters (2-μm pore diameter) were used as impaction substrates in the MOI. The first three stages were coated with approximately 2 mg of dimethylpolysiloxane (Dow Corning 200 Fluid) to reduce particle bounce and re-entrainment. Samples were collected twice daily, following a diurnal cycle, with daytime samples collected from 0800 to 1800 h, and nighttime samples from 2200 to 0600 h the following morning. The NRI was operated simultaneously during two of the eight MOI sampling periods, using similarly coated Gelman Zefluor Teflon filters as impaction substrates. Fifteen field blank substrates were collected to monitor potential contamination experienced while loading and unloading the MOI and while placing the sampler in the sampling position.

All of the samples were collected on board the U.S. Environmental Protection Agency's RV *Lake Guardian* while it was anchored into the wind at one of three positions offshore the Chicago/Gary area (see Figure 1 and Table 1). Samplers were placed at the bow to avoid contamination by exhaust from the ship's diesel engines or other particle-producing activities.

Deposition samples were collected on 10-cm diameter coated Gelman Zefluor Teflon filters mounted on the airfoils. Depositing particles were collected over 3-day periods to ensure collection of adequate mass for analysis, and therefore, only two samples were collected during this experiment. The first sample was collected from July 21 to July 25 while the ship was located first at site 1 and later at site 5. The second sample was collected from July 25 to July 28 at sites 5, 1, and 0.

TABLE 1. Sampling Schedule, Locations, and Average Meteorological Parameters

	sampling period 1	
date	July 21−23	July 24−25
ship location	site 1	site 5
time exposed (h)	37	21.0
average		
air temp (°C)	22.2	22.2
water temp (°C)	21	22
relative humidity (%)	86	83
wind speed (m s^{-1})	4.7	3.3
wind direction (deg); Chicago	264	271
wind direction (deg); lake	240	203

	sampling period 2		
date	July 25	July 26	July 27−28
ship location	site 5	site 1	site 0
time exposed (h)	10.2	14	35.2
average			
air temp (°C)	23.1	23.4	20.0
water temp (°C)	22	22	22
relative humidity (%)	77	68	80
wind speed (m s^{-1})	4.8	3.0	5.7
wind direction (deg), Chicago	264	37	137
wind direction (deg), lake	280	165	84

Wind speed, relative humidity, and air temperature were measured at 10-s intervals onboard the RV *Lake Guardian*, and their 5-min averages were recorded during the entire campaign. Sample averages of these parameters are listed in Table 1 for each of the three different Lake sampling locations and for each of the two samples, and summaries of these parameters are contained in Figure 2.

Heading-corrected wind direction was manually recorded hourly by the ship's crew members. Wind direction was also measured at a shoreline site located on the Illinois Institute of Technology (IIT) campus approximately 1.6 km inland. Average wind direction at each site, as measured both at IIT and by the ship's crew, are listed in Table 1. Figure 3 graphs frequency versus direction from which the wind came as measured at the IIT site. As shown there, winds were from the Chicago area >80% of the first sampling period, with the remaining 20% from the east. The second sampling period saw winds more evenly divided between the Chicago area to the west and northwest (39%) and the northern lake and rural eastern shore (61%), with no winds seen from the industrialized area near Gary, IN, to the south.

Elemental Analyses. All of the impactor and deposition samples and 30 MOI laboratory and field blanks (21 uncoated and 9 coated) were analyzed for up to 48 elements by Instrumental Neutron Activation Analysis (INAA) using techniques described previously (*14*). Additionally, the MOI samples and blanks were analyzed for up to 41 elements by X-ray fluorescence (XRF) at the EPA's Laboratory for Source Apportionment in Research Triangle Park, North Carolina. Analyses for eight species (As, Ca, Mg, S or SO_4^{2-}, Sb, Se, V, and Zn) were used in the deposition velocity calculations described below. Calcium, Mg, and V were determined by INAA from γ-ray spectra acquired for 7.5 min on intrinsic Ge detectors with efficiencies (relative to 3 $\times$ 3 NaI) between 20 and 40% after a 10-min irradiation at a flux of 4×10^{13} n cm^{-2} s^{-1} in the University of Missouri Research Reactor in Columbia, MO. Arsenic, Sb, Se, and Zn were determined from γ-ray spectra acquired with similar detectors at the

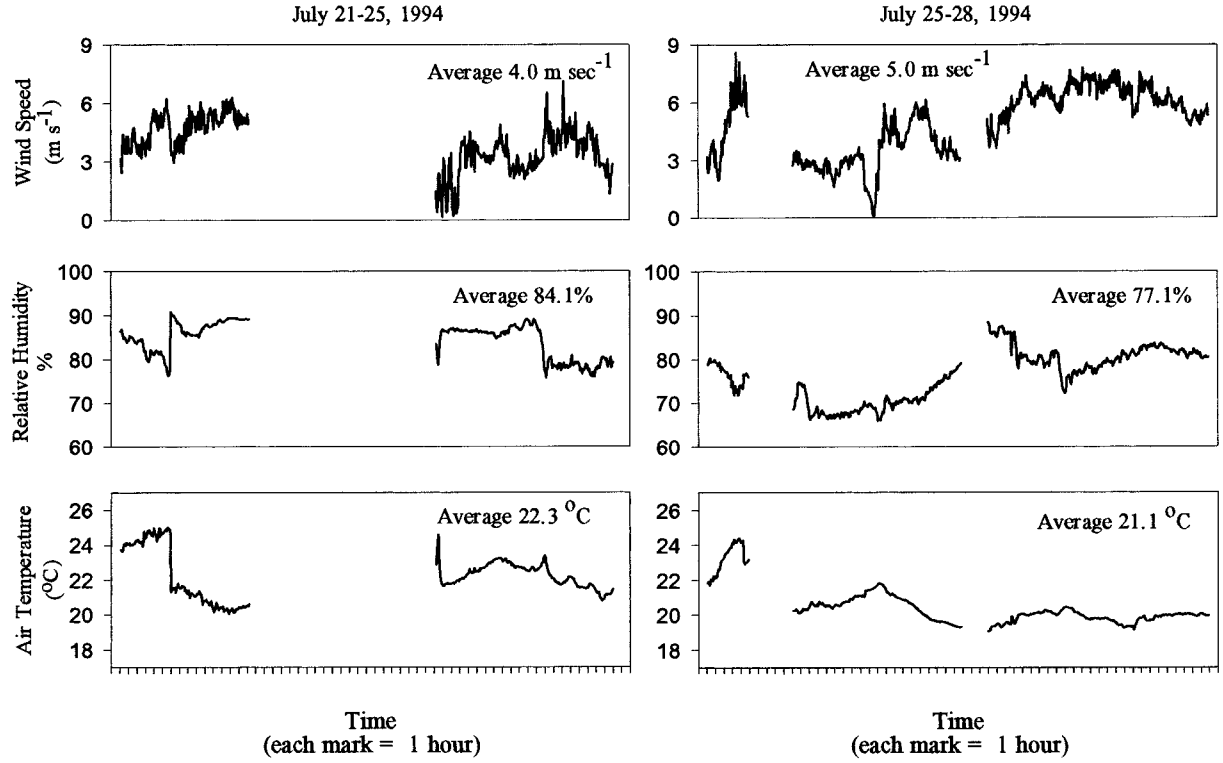

FIGURE 2. Plots of 5-min averages of wind speed, relative humidity, and air temperature collected aboard the RV *Lake Guardian* during two sampling periods. Gaps indicate missing data.

TABLE 2. Sample-to-Blank Ratios

		MOI		
element	flux plates	max	av	NRI[a] av
As	4.2	330	16	38
Zn	4.9	41	7.7	21
Se	5.8	37	5.5	2.7
Sb	9.7	76	15	23
Ca	35	590	33	283
Mg	7.1	72	8.1	39
V	6.8	41	4.9	18

[a] Average of stages C and D only.

University of Maryland for up to 24 h from 3 to 30 days after a single 4-h irradiation at a flux of 7.5×10^{13} n cm^{-2} s^{-1} in the Brookhaven National Laboratory's High Flux Beam Reactor in Upton, NY. Sulfur was determined in the MOI samples by XRF. Sulfur was measured as SO_4^{2-} by ion chromatography in the deposition flux samples, extracted with 3 mL of mineral spirits and 12 mL of Ultrapure water for approximately 3 min. The mineral spirits component of this solution was then evaporated on a hot plate, and the remaining sample was weighed and a portion (2 mL) injected into a Dionex series 4500 ion chromatograph (IC) using an AS4A column for sulfate quantification. Neither S nor sulfate concentrations were measured in NRI samples. Results for each of the eight species are listed in Tables 3and 4.

All measurements were corrected for substrate blank concentrations. Analyses of 15 field blank substrates were indistinguishable from laboratory blanks. Therefore, these were averaged along with laboratory blank values before correcting the samples. As shown in Table 2, average sample-to-blank (S:B) ratios (calculated as the ratio of the uncorrected value to the average blank concentration) for the flux measurements ranged from 4.2 for As to 36 for Ca. As more mass was collected by the impactors, S:B ratios for the MOI and NRI were greater than those for deposition plates for all elements. Table 2 lists the maximum MOI ratio, i.e., the S:B ratio for each stage that contained the peak mass of each element, as well as the arithmetic average S:B ratio across all nine stages. The maximum S:B ratios exceed 36 for all elements determined in MOI samples. The NRI S:B ratios are the average of stages C and D, as only these two stages were used in the deposition velocity calculations that follow. The S:B ratio for Se in NRI samples was 2.7, i.e., lower than that of the flux plate. However, Se is almost exclusively associated with fine particles, and it was undetected on one NRI stage in each of the two samples used here. Sulfur was undetected in the XRF laboratory and field blank filters; therefore, the S values as determined by XRF needed no blank correction, and their S:B ratios are not listed in Table 2.

Williams Model. Dry deposition velocities to a smooth surface were calculated using an adaptation of the Williams model (*16*). The Williams model is designed to predict dry deposition velocities of particles to water surfaces, and accounts for the effects of wave-breaking and particle growth from increased humidity near the water surface. The model calculates particle-size-dependent V_d values based on atmospheric stability (which is a function of water/air temperature difference), wind speed, and relative humidity. In general, particles $>0.4\,\mu$m are most affected by sedimentation and inertial forces. Here V_d values increase rapidly with increasing particle size, especially in the supermicrometer region where particle V_d values are comparable to their terminal settling velocities and increase with the square of particle diameter. Below 0.4 μm, Brownian diffusion increases V_d values inversely with particle size. The result is predicted to be a smooth curve with a minimum V_d near 0.4 μm. Furthermore, the curve is shifted upward at higher wind speeds and for greater instability, especially in the region of the minimum. To simulate deposition to a smooth, dry, plate, the model was run to neglect both particle growth at the water surface and the breaking-wave effect. The 5-min averaged ambient temperature and wind speed data measured on the RV *Lake Guardian* were used as inputs, and

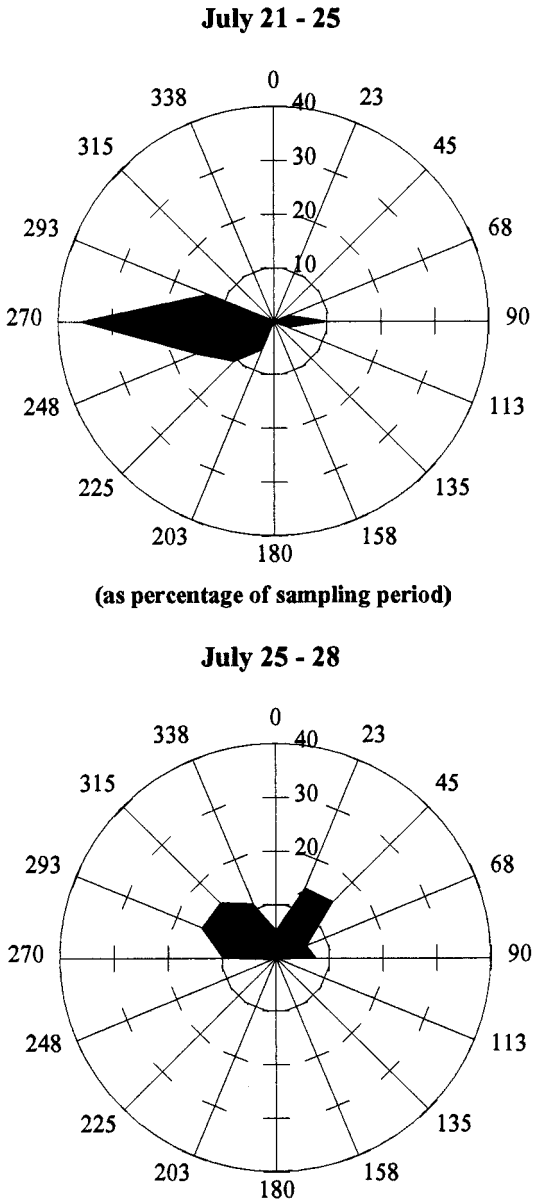

FIGURE 3. Wind direction frequency spectra for the measurement periods. Values give direction from which winds traveled.

data from the two sampling periods were modeled separately. An average surface water temperature of 21.5 °C was used in the stability calculations, as measured on site during sampling (*20*).

Results and Discussion

Elemental Fluxes and Size Distributions. Dry deposition fluxes (F_i), in mg m^{-2} h^{-1}, were calculated from elemental masses (m_i) as follows and are listed in Table 3:

$$F_i = \frac{m}{At}$$

where A is the area of the deposition substrate and t is the time of exposure.

Individual impactor stage aerosol concentrations, in ng m^{-3}, are listed in Table 4. Elemental concentrations measured during the first sampling period (July 21−24) all exceeded those of the second period. During the former, the samplers experienced winds from the Chicago area for >80% of the time, with the remaining winds bringing cleaner air down and across the lake from the northeast (see Figure 3). During the latter period, polluted Chicago winds were only experienced for 39% of the time. The reduced concentrations for all elements during the second period indicate that the elevated urban and industrial ambient concentrations can be readily measured above background. During the first period, As and Sb concentrations were >2- and >4-fold greater than their concentrations in the second period. With the exception of S, flux measurements showed a similar trend (Table 3), with elemental fluxes ranging from 2- to 4-fold greater during the first period.

TABLE 3. Elemental Dry Deposition Fluxes Measured from Airfoil Surrogate Surfaces in This Work and Estimated by Pirrone et al. (μg m^{-2} h^{-1})

	July 21−25		July 25−28		Pirrone et al.
	flux	σ^b	flux	σ^b	PM10 flux[a]
As	0.0048	0.0004	0.0027	0.0005	
Ca	58.7	5.2	21.7	7.5	5.9
Mg	14.2	1.7	7.39	1.78	
S	2.83	0.47	7.83	1.03	1.25
Sb	0.0100	0.0002	0.0045	0.0007	
Se	0.0058	0.0009	0.0021	0.0007	0.025
V	0.056	0.003	0.019	0.004	
Zn	0.992	0.081	0.266	0.081	0.088

[a] Particles with aerodynamic diameters smaller than 10 μm. [b] Analytical uncertainty expressed as 1 standard deviation.

Pirrone et al. (*21*) used a hybrid receptor modeling approach to estimate average, lakewide, elemental dry deposition fluxes of various elemental constituents of aerosol particles <10 μm. Their model used air mass trajectory/dispersion calculations to derive spatial profiles of airborne pollutant concentrations and a Williams-type model to calculate deposition fluxes. The latter included the effects of wind speed, stability, wave height, particle size, and hygroscopic growth occurring above and near the water surface. However, particle-size distribution parameters used in the model were derived from literature and not measured. As indicated in Table 3, fluxes reported herein for Ca and Zn depositing to southern Lake Michigan exceed the lakewide averages of Pirrone et al. (*21*) by 10-fold, despite the fact that the former represent minimum fluxes, i.e., because they were determined under stable, low-wind conditions and because they are appropriate for smooth dry surfaces. The >10-fold differences in these estimates likely reflect the extended particle-size range encompassed in our study and the fact that strong concentration (and hence) flux gradients are observed for large particles carried across the lake. Interestingly, their lakewide flux for Se, an element for which our measurements show very little residence in supermicrometer particles, was 4-fold greater than our (southern Lake) Se flux. This is attributable to their much larger allocation of Se mass to supermicrometer particles.

Size distributions for each of the two observation periods are plotted in Figure 4 in which the arithmetic average of the impactor data for samples collected during each deposition flux measurement period are normalized to the logarithmic bin width and plotted against the aerodynamic midpoint diameter. As the MOI and NRI size intervals overlap at sizes >6.5 μm, only the top two stages (C and D) of the NRI are used in combination with the MOI data. Also in a few of the MOI samples used herein, the backup filters, which usually contain negligible amounts of mass, were visibly contaminated by blow-back from the rotary-vane pump located immediately downstream. These data were therefore discarded. Uncontaminated backup filters collected in the study showed negligible mass. Only one NRI sample was collected

TABLE 4. Elemental Impactor Concentrations and Analytical Uncertainties[a] (ng/m³)

impactor stage	As		Ca		Mg		S		Sb		Se		V		Zn	
	concn	σ	concn	σ	concn	σ	concn	σ	concn	σ	concn	σ	concn	σ	concn	σ
July 21–25																
NRI D	0.0161	0.00059	120	12	12.0	43	ND		0.0165	0.00046	0.00270	0.00038	0.0727	0.0037	1.74	0.12
NRI C	0.0071	0.00082	47.5	21	4.6	13	ND		0.00015	0.00062	ND		0.0382	0.0013	0.61	0.20
MOI 0	0.0334	0.0051	202	22	51.4	5.8	16.7	5.1	0.0222	0.0062	0.050	0.010	0.198	0.022	3.09	0.54
MOI 1	0.0964	0.0068	479	52	118	12	78.1	11	0.126	0.0093	0.069	0.018	0.726	0.043	17.6	1.4
MOI 2	0.0486	0.0050	59.4	7.7	27.3	5.7	27.2	5.8	0.0731	0.0067	0.096	0.014	0.288	0.024	13.3	1.1
MOI 3	0.0351	0.0056	21.6	4.6	8.77	4.7	80.3	11	0.105	0.0062	0.113	0.020	0.206	0.019	19.5	1.4
MOI 4	0.0538	0.0061	8.10	3.5	4.84	2.9	242	30	0.154	0.0070	0.392	0.034	0.113	0.016	13.5	1.1
MOI 5	0.172	0.0080	2.82	2.3	2.81	2.8	290	34	0.264	0.0077	0.590	0.042	0.246	0.019	8.85	0.75
MOI 6	0.133	0.0069	1.04	2.7	1.75	2.0	129	16	0.184	0.0064	0.194	0.021	0.111	0.014	3.11	0.44
MOI 7	0.0968	0.0064	ND		1.18	2.0	74.5	10	0.112	0.0059	0.101	0.016	0.021	0.013	1.25	0.38
MOI 8	0.0383	0.0054	ND		2.76	2.4	21.5	5.1	0.0324	0.0052	0.026	0.014	0.044	0.015	0.51	0.36
July 25–28																
NRI D	0.00700	0.00021	81.9	8.4	36.3	2.5	ND		0.00490	0.00020	ND		0.0385	0.0031	0.644	0.046
NRI C	0.00530	0.00043	30.8	3.1	13.5	3.8	ND		0.00220	0.00032	0.00086	0.00050	0.0211	0.0046	0.190	0.075
MOI 0	0.0083	0.0039	56.5	7.4	23.4	4.2	4.75	4.3	0.0121	0.0050	ND		0.036	0.018	2.68	0.54
MOI 1	0.0452	0.0055	218	25.	71.0	9.1	26.2	5.9	0.0601	0.0058	0.013	0.011	0.148	0.023	6.03	0.75
MOI 2	0.0177	0.0042	45.1	6.1	15.6	3.5	11.1	4.2	0.0262	0.0045	0.0040	0.0083	0.044	0.019	2.27	0.53
MOI 3	0.0088	0.0055	15.9	3.5	4.71	2.1	11.4	4.2	0.0203	0.0055	0.009	0.017	0.034	0.013	5.56	0.60
MOI 4	0.0178	0.0056	2.47	2.4	1.56	2.0	37.3	6.3	0.0790	0.0056	0.041	0.019	0.009	0.012	2.75	0.46
MOI 5	0.0671	0.0062	ND		1.48	2.1	155.	19.	0.0771	0.0059	0.143	0.018	0.090	0.014	3.52	0.48
MOI 6	0.0374	0.0052	0.93	2.4	ND		76.0	10.	0.0501	0.0052	0.058	0.016	0.248	0.019	2.75	0.42
MOI 7	0.0212	0.0051	0.12	2.5	1.29	1.9	34.8	6.1	0.0377	0.0052	0.025	0.018	0.159	0.015	0.70	0.34
MOI 8	0.0039	0.0051	1.91	2.4	1.81	2.2	8.30	4.6	0.0603	0.0093	ND		0.001	0.012	0.23	0.35

[a] Analytical uncertainty expressed as 1 standard deviation (σ). [b] ND, none detected.

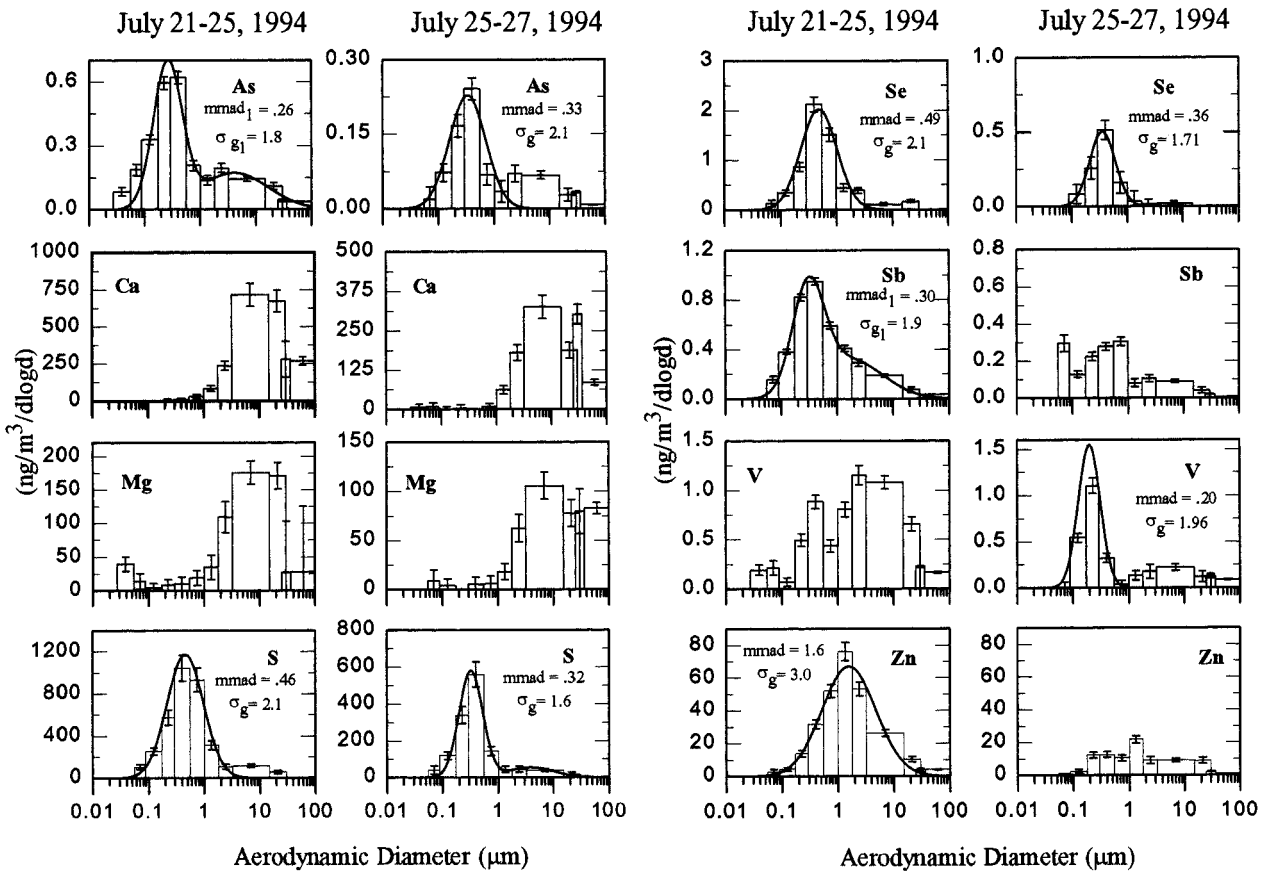

FIGURE 4. Size spectra of particles bearing various elements, plotted as concentration (in ng m^{-3}), normalized to the logarithmic bin width, versus aerodynamic impactor midpoint diameter, for stages 0–8 of the micro-orifice impactor and stages C and D of the Noll Rotary impactor. Mass median aerodynamic diameters (mmad) and geometric standard deviations (σ_g) are listed for distributions that could be fitted with log-normal distribution functions. Geometric mass mean aerodynamic diameters (gmmad) are listed for spectra which could not be fitted. Subscripts indicate that size distribution parameters listed correspond to the fine particle mode.

during each of the two observation periods, while five and three MOI samples were collected during the first and second periods, respectively. The NRI concentrations were multiplied by factors of 0.4 and 0.33, respectively, for the two periods to account for lower coarse particle concentrations during the periods in which the NRI was not operated. These

TABLE 5. Results of Deposition Velocity Model Calculations

midpoint diameters		July 21−25			July 25−28		
aerodynamic (μm)	physical[a] (μm)	multi-element tracer[b] (cm s^{-1})	σ	Williams model (cm s^{-1})	multi-element tracer[c] (cm s^{-1})	σ	Williams model (cm s^{-1})
60.40	42.7	10.98	0.041	11.05	10.97	0.029	11.10
30	21.2	2.67	0.143	2.77	2.69	0.028	2.87
21.20	15.0	1.35	0.023	1.39	1.34	0.016	1.49
6.92	4.90	0.144	0.0093	0.150	0.143	0.0046	0.150
2.40	1.70	0.0228	0.0183	0.020	0.0198	0.0185	0.021
1.34	0.949	0.0180	0.0207	0.0077	0.0160	0.0513	0.0088
0.74	0.525	0.0073	0.0075	0.0041	0.0117	0.0460	0.0056
0.40	0.282	0.0043	0.0038	0.0037	0.0081	0.0150	0.0060
0.22	0.158	0.0052	0.0049	0.0048	0.0089	0.0106	0.0083
0.12	0.087	0.0059	0.0054	0.0075	0.0130	0.0167	0.0132
0.07	0.049	0.0054	0.0100	0.0121	0.0160	0.0160	0.0215

[a] Calculated assuming a particle density of 2 g cm^{-3}. [b] Initial guesses in order of decreasing particle diameter were 11.1, 2.7, 1.4, 0.15, 0.019, 0.007, 0.003, 0.002, 0.002, 0.003, and 0.005 cm s^{-1}. [c] Initial guesses in order of decreasing particle diameter were 10.9, 2.8, 1.4, 0.15, 0.02, 0.008, 0.005, 0.004, 0.006, 0.01, and 0.015 μm.

factors were calculated as the averages of the concentration ratios of the top stage of the MOI from the period the NRI was operating to those for the period in which it was not operating. The adjusted values are used in the distributions plotted in Figure 4 and represent a continuation of the average distributions up to 100 μm. Size distribution parameters, i.e., mass median aerodynamic diameter (mmad) and geometric standard deviation (σ_g), were calculated for each element using the method of Dzubay and Hasan (*22*) and are displayed in Figure 4. Their method uses efficiency curves to fit the mass concentrations for individual impactor stages with the sum of up to three log-normal distribution functions (LNDF). A nonlinear least-squares method is used to minimize a reduced χ^2. Herein, impactor efficiency data used in the calculations are reported in Ondov and Divita (*23*) and up to two LNDFs were fit to the data. For spectra not fit with a LNDF, the geometric mass mean aerodynamic diameter (gmmad) and σ_g were calculated and are displayed in Figure 4.

As shown in Figure 4, As, S, Se, and Sb were primarily associated with fine particles, whereas Ca and Mg were mainly associated with coarse particles. The spectra for As, Sb, V, and to a lesser extent S were bimodal and contained both coarse and fine aerosol modes, wherein 38, 44, 74, and 13% of the mass was contained in coarse particles during the first period. Mass median aerodynamic diameters for fine-particle peaks in spectra developed for the first period were 0.26, 0.30, 0.46, 0.49, and 0.40 μm for As, Sb, S, Se, and V respectively. Those for S, Se, and V (i.e., 0.32, 0.36, and ~0.4, respectively) were somewhat smaller in the second period, whereas the mmad for As appears to be shifted to a slightly larger value in the second period. Zinc exhibited a mmad of 1.6 μm during the first period, and while its concentration was too low to obtain an mmad by fitting its spectrum with a LNDF, the gmmad, (i.e., 1.8 μm) was determined for Zn aerosol sampled during the second period. The mmad and gmmad are identical when the distribution is unimodal and the population is log-normally distributed. Calcium and Mg concentrations peaked on coarse particles of aerodynamic diameter ~10 μm.

Chemical Mass Balance Deposition (CMBD) Model. Individual dry deposition velocities were calculated by equating calculated and measured fluxes for each element, wherein the calculated fluxes are the sum of the products of the dry deposition velocity, $V_{d,j}$ (appropriate for particles collected on each of the j impactor stages), and the mass concentration, C_i, for each element, i, i.e.

$$F_i = \sum_{j=1}^{11} (V_d C_i)_j \quad (1)$$

One expression of the form of eq 1 can be written for each of the elements determined in both aerosol and deposition samples. If we assume that V_d values are not affected by differences in the composition of particles bearing the various elements (which may, in fact, represent different particle populations, i.e., from different sources), then the j V_d values may be determined by solving the system of j equations. Particle densities may, in fact, differ by as much as 50%, which could account for an error of 19% in deposition velocities. However, we regard this to be tolerable in view of the 200−300% uncertainties in fine-particle deposition velocities.

To achieve the best results, we chose to include in the model elements for which the analytical value was >3 times its uncertainty in both deposition and aerosol particulate samples. Furthermore, to obtain good solutions for submicrometer-particle V_d values, it was necessary to include elements associated with both fine and coarse particles. These criteria were met by As, Ca, S, Se, Sb, and Zn for the first period and As, Mg, Sb, V, and Zn for the second period. Thus sets of six and five equations could be constructed for the two each periods, respectively.

The solutions to each set of equations were determined by iterative solution using the Levenberg−Marquardt method (*24*). The method simultaneously solves for multiple unknowns and requires a set of j initial "guesses", i.e., one for each size interval. Herein, we attempted solutions for 11 size intervals. Solutions for particles <3.2 μm were constrained such that $V_{d,j} > 0$. Those for particles >3.2 μm were constrained to values >90% of their terminal settling velocities (V_{ts}) calculated for a particle density of 2 g cm^{-3}. Initial "guesses" for the V_d values were calculated with the Williams model using a lower (by 0.5 m s^{-1}) wind speed and higher stability (T_w = 20 °C) than experienced in either of the two periods. Initial guesses determined in this manner were designed to be less than likely solutions for submicrometer particles and approximately equal to the terminal settling velocities of the supermicrometer particles. To determine sensitivity to variations in the set of initial guesses, the model was rerun with another set of initial guesses wherein those for submicrometer particles were chosen to be 2-fold greater. Although desirable, the method does not require that the number of linear equations equal the number of unknowns. Herein, physically significant solutions are achieved by imposing constraints, provided that supermicrometer particle V_d values are reasonably estimated by the William's model.

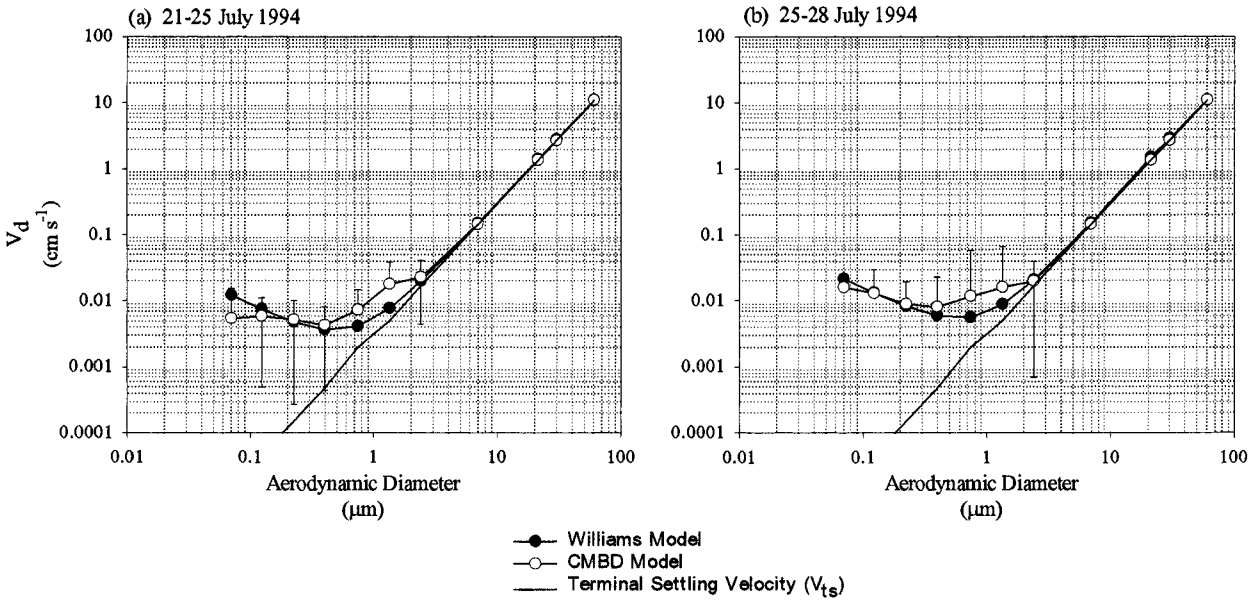

FIGURE 5. Deposition velocity versus particle size curves derived from CMPD and Williams models. Results calculated for the first sampling period (a) used As, Ca, S, Sb, Se, and Zn data. Those for the second sampling period (b) used As, Mg, Sb, V, and Zn data.

The calculated $V_{d,j}$ values for each of the two periods are listed in Table 5 and shown in Figure 5, wherein $V_{d,j}$ is plotted versus the midpoint aerodynamic diameter for each impactor stage. Also listed in Table 5 are the midpoint aerodynamic and physical diameters as well as values of $V_{d,j}$ values calculated for the meteorological conditions of each period with the Williams model as described above. Initial guesses are listed at the bottom of Table 5. Physical diameters were estimated from the aerodynamic diameters as described in Hinds (*25*) using densities of 2 g cm^{-3} for both submicrometer and supermicrometer particles.

Uncertainties in the individual $V_{d,j}$ values were estimated with the Monte Carlo method. Specifically, the CMBD model was run using >30 000 sets of input data in which each set was perturbed by adding Gaussianly distributed random deviations to each of the input data points. The standard deviation used to describe the Gaussian distribution for each input was taken to be the standard deviation of the individual measurements. For impactor samples collected in the first period, these typically ranged from 3 to 7% for peak stages containing As, Se, Sb, V, and Zn and from 10 to 12% for Ca, Mg, and S. Uncertainties in m_i values collected on deposition plates ranged from 2% for Sb to 16% for S (see Table 3).

Model Results. As shown in Figure 5, V_d curves calculated with the CMBD model exhibit the expected behavior with respect to particle size. Deposition velocities for particles with aerodynamic diameters >2 μm are nearly identical with their terminal settling velocities. Those for particles <2 μm are typically 2.5-fold greater than the initial guesses entered into the model for the first period and 1.5−2-fold greater in the second period. In both plots, minima in the V_d curves are evident in the 0.2−0.4 μm region.

Another indication of model performance is obtained by comparing the fluxes calculated from the modeled V_d values and the measured fluxes. Ratios of the former to the latter for each element are contained in Figure 6. During the first period, ratios for Sb, Se, Zn, and Ca ranged from 0.74 to 1.1, whereas As is overpredicted by 2-fold, and S is underpredicted by a similar factor. Ratios for the second period were similar for Sb, As, and V, but somewhat greater for Zn (1.7). Magnesium is measured more poorly than Ca by INAA, and its ratio was 2.3.

Monte Carlo calculations suggest that the uncertainties in the V_d values for particles with aerodynamic diameters >3 μm were small, ranging from 0.4 to 6%. However, those for particles <3 μm are comparable to their mean values and are roughly 2σ greater than their initial guesses. This suggests that this is the minimum level for which the CMBD model is capable of providing a solution for fine particles, given the levels of uncertainty in the input data used herein. It is noteworthy that the solutions for fine particles were insensi-

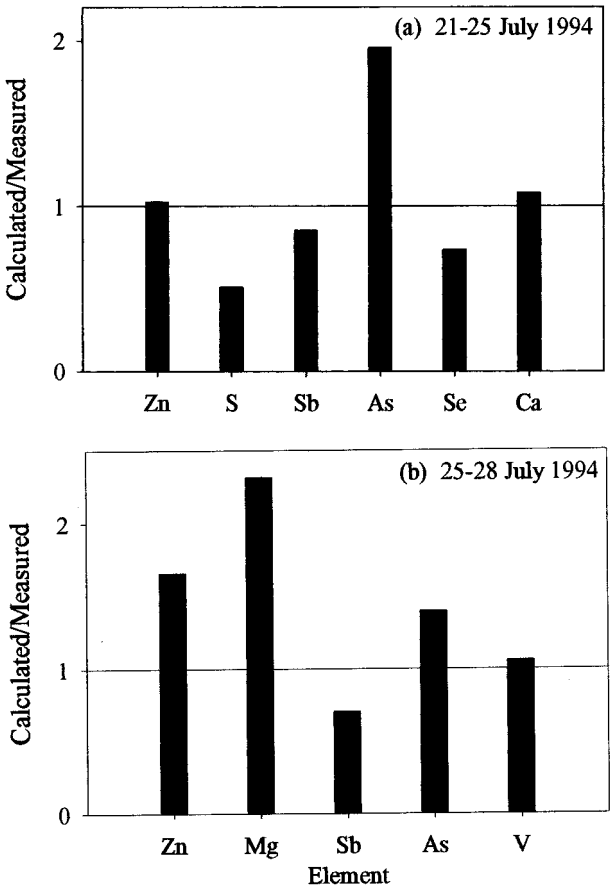

FIGURE 6. Comparison of fluxes measured with surrogate surfaces with those calculated using deposition velocities derived from the CMBD model.

tive to variations in the initial guess. For example, they were essentially identical to those reported in Table 5 when initial guesses were 2.5-fold larger. Last, uncertainties were largest for the smallest size interval as this interval contained so little mass. Likewise, those for the second period exceeded those of the first period, as the sample mass loadings were significantly lower during this period and analytical uncertainties were correspondingly higher.

Deposition velocities determined from the CMBD model agree well with those determined from the Williams model. This is not surprising for supermicrometer particles whose V_d values are dominated by settling and are therefore readily measured. But this was true even for fine particles for which V_d values are thought to be limited by transfer through a viscous sublayer of poorly known extent. As shown in Figure 5, deviations from the Williams model V_d values were largest between 0.4 and 1.4 μm, where CMBD values were from 1.2- to 2.5-fold greater in the first period and from 1.3 to 2.1 greater in the second period. Nevertheless, both Williams and CMBD models predict larger submicrometer V_d values for the second period, as expected for the higher wind speeds and less stable conditions present during this period (see Figure 2).

Deposition velocities described herein were determined under stable atmospheric conditions, i.e., those unfavorable to dry deposition. It is likely, therefore, that more accurate values could be obtained under more unstable or turbulent conditions favoring dry deposition when collection of more mass in shorter periods would improve measurement accuracy and calculated deposition velocities would be more distinguishable from model residuals (i.e., noise). Despite their large uncertainties, the values reported herein are an improvement on those reported using other techniques (*10*). By microscopy, V_d values for particles in two submicrometer size intervals, i.e., 0.37 and 0.77 μm, were 0.03 and 0.0066 cm s^{-1}, respectively, but uncertainties were 10 times the mean. Reconciliations between measured and calculated fluxes determined here are generally better than achieved previously with the multistep Sehmel−Hodgson model in which only coarse-particle components were considered (*8*).

Acknowledgments

This work was supported by the U.S. Environmental Protection Agency, Grant CR 822046-01, Great Waters Program. We would like to thank Dr. Tom Holsen and his group at the Illinois Institute of Technology for providing the NRI samples used in this work, and we gratefully acknowledge the crew of the RV *Lake Guardian* for their assistance with the field sampling.

Literature Cited

(1) Zufall, M. J.; Davidson, C. I.; Caffrey, P. F.; Ondov, J. M. *Environ. Sci. Technol.* **1988**, *32*, 1623−1628.

(2) Eisenreich, S. J. *Water, Air, Soil Pollut.* **1980**, *13*, 287.

(3) Schmidt, J. A.; Andren, A. A. In *Toxic Contaminants in the Great Lakes*; Nriagu, J. O., Simmons, M. S., Eds; John Wiley & Sons: New York, 1984; Vol. 14.

(4) Strachan, W. M. J.; Eisenreich, S. J. In *The Workshop on the Estimation of Atmospheric Loadings of Toxic Chemicals to the Great Lakes Basin*: International Joint Commission: 1988; Appendix I.

(5) Dolske, D. A.; Sievering, H., *Water, Air, Soil Pollut.* **1979**, *12*, 485.

(6) Wu, Z. Y.; Han, M.; Lin, Z.-C.; Ondov, J. M. *Atmos. Environ.* **1994**, *28*, 1471.

(7) Sievering, H.; Boatman, J.; Luria, M.; Van Valin, C. C. *Tellus* **1989**, *41B*, 338.

(8) Holsen, T. M.; Noll, K.; Fang, G.; Lee, W.; Lin, J.; Keeler, G. J. *Environ. Sci. Technol.* **1993**, 27, 1327.

(9) Wu, Y.-L.; Davidson, C. I.; Dolske, D. A.; Sherwood, S. I. *Aerosol Sci. Technol.* **1992**, *16*, 65.

(10) Davidson, C. I.; Wu, Y.-L. In *Acid precipitation, sources, deposition, and canopy interactions*; Lindberg, S. E., Page, A. L., Norton, S. A., Eds.; Springer-Verlag: New York, 1989; Vol. 3.

(11) Nicholson, K. W. *Atmos. Environ.* **1988**, *22*, 2653.

(12) Zufall, M. J.; Davidson, C. I. In *Atmospheric Deposition of Contaminants to the Great Lakes and Coastal Waters;* Baker, J. E., Ed.; SETAC: Pensacola, FL, 1996.

(13) Zufall, M.; Bergin, M. H.; Davidson, C. I. *Environ. Sci. Technol.* **1998**, *32*, 584−590.

(14) Ondov, J. M.; Dodd, J. A.; Tuncel, G. *Aerosol Sci. Technol.* **1990**, *13*, 249.

(15) Caffrey, P. F.; Suarez, A. E.; Ondov, J. M.; Han, M. *J. Aerosol Sci.* **1996**, *27*, S3.

(16) Williams, R. M. *Atmos. Environ.* **1982**, *16*, 1933.

(17) Wu, Y.-L.; Davidson, C. I.; Russell, A. G. *Aerosol Sci. Technol.* **1992**, *17*, 231.

(18) Marple, V. A.; Rubow, K. L.; Behm, S. M. *Aerosol Sci. Technol.* **1991**, *14*, 434.

(19) Noll, K. E.; Pontius, A.; Frey, R.; Gould, M. *Atmos. Environ.* **1990**, *24A*, 903.

(20) Baker, J. E. Chesapeake Biological Laboratory, Solomons, MD, personal communication, 1994.

(21) Pirrone, N.; Keeler, G. J.; Holsen, T. M. *Environ. Sci. Technol.* **1995**, *29*, 2112.

(22) Dzubay, T. G.; Hasan, H. *Aerosol Sci. Technol.* **1990**, *13*, 144.

(23) Ondov, J. M.; Divita, Jr., F., *J. Radioanal. Nucl. Chem.* **1993**, *167* (2), 247.

(24) More, J. J.; Barbow, B. S.; Hillstrom, K. E. *Users Guide to MINIPACK I, ANL 80-74*; Argonne National Laboratory, 1980.

(25) Hinds, W. C. *Aerosol Technology−Properties, Behavior, and Measurement of Airborne Particles*; John Wiley & Sons: New York, 1982.

Received for review July 23, 1997. Revised manuscript received February 10, 1998. Accepted February 19, 1998.

ES970644F